

## Bootstrap of Pion-Pion Scattering in the Unitarized Strip Approximation

P. D. B. COLLINS

*Physics Department, University of Durham, Durham City, England*

AND

R. C. JOHNSON\*

*Physics Department, University of Toronto, Toronto 5, Canada*

(Received 4 March 1969)

We give the result of a bootstrap of the  $\rho$  and Pomeranchuk trajectories in pion-pion scattering, using the unitarized strip approximation. In this scheme, we construct an analytic, crossing-symmetric, unitary amplitude with Regge asymptotic behavior. This is achieved by starting with strips in which the double spectral function is parametrized by Regge poles, in the way devised by Chew and Jones, and adding the elastic double spectral functions in each channel calculated by the Mandelstam iteration method. Unitarity is imposed using the  $N/D$  method with inelasticity. We find self-consistent trajectories which bear a fair resemblance to those found experimentally, at least for small  $|t|$ , and obtain a  $\rho$  of width 155 MeV, which is very much better than earlier calculations. This and related improvements are due to the proper inclusion of Pomeranchon exchange. The requirement of self-consistency does not fix the trajectories uniquely, but the range of solutions is comparatively narrow, with  $0.32 \leq \alpha_\rho(0) \leq 0.69$ . There are still some unsatisfactory features in comparison with the phenomenological trajectories: We always find that  $\alpha_\rho(\infty) > -1$ , there is a too rapid increase of  $\text{Im}\alpha$  just above threshold, and the trajectories do not rise much above  $\text{Re}\alpha=1$ . We draw some conclusions about the prospects for this sort of  $S$ -matrix dynamics.

### I. INTRODUCTION

IN a previous paper<sup>1</sup> we have described a method of carrying out bootstrap calculations using "the unitarized strip approximation."<sup>2</sup> In this model we parametrize the asymptotic strip of the double spectral functions by Regge poles, in the way devised by Chew and Jones,<sup>3</sup> and then use the Mandelstam<sup>4</sup> iteration method to calculate the nearby parts of the elastic double spectral functions in each channel. These are the corners of the double spectral functions shown in Fig. 1 of Ref. 1. The sum of the strip and corner contributions to both the left- and right-hand cuts of the  $s$ -channel partial-wave amplitudes are calculated, and unitarity is imposed by the Frye-Warnock<sup>5</sup> inelastic  $N/D$  equations. A parameter search is then undertaken to try and make the input Regge functions coincide with the output Regge functions generated by the  $N/D$  equations. If they can be made consistent a bootstrap of the trajectories has been achieved.

The advantages of this model over earlier calculations,<sup>6,7</sup> using the "new strip approximation" of Chew and Jones,<sup>3</sup> are that by including the corners of the double spectral functions we automatically include

higher Born approximations to the amplitude in the left-hand cut of the partial-wave amplitudes. (The first Born approximation, i.e., "the potential," consists of the  $t$ - and  $u$ -channel strips.) It has been shown<sup>8</sup> that it is essential to include such higher Born approximations in nonrelativistic potential-scattering calculations, and we might expect that this will also be the case in  $S$ -matrix theory. Their inclusion is particularly important when there are repulsive potentials, and we know that the Pomeranchuk ( $P$ ) trajectory gives rise to a repulsive potential.<sup>9</sup> At the same time a knowledge of the elastic double spectral functions enables us (by crossing symmetry) to calculate the inelasticity in the  $s$ -channel strip region, and this inelasticity can be included in the Frye-Warnock  $N/D$  equations.

In Ref. 1 we used this method to bootstrap the  $\rho$  trajectory in the  $\pi$ - $\pi$  scattering amplitude, and were able to obtain self-consistent trajectories. Since, however, the  $\rho$ -exchange force also generated a  $P$  trajectory which was not included in the input, the bootstrap was incomplete.

In this paper we describe a bootstrap of the  $\rho$  and  $P$  together. This was not really possible in the new strip approximation because the  $P$  repulsion prevented solution of the  $N/D$  equations unless a rather doubtful "normalization" procedure was used.<sup>7,10</sup> On iterating the potential, this difficulty is overcome, and good self-consistent trajectories are obtained.

Also in Ref. 1 the parametrization of the Regge functions was unsatisfactory since in order to generate suitable trajectories  $\alpha(t)$ , a large peak in  $\text{Im}\alpha(t)$  was needed

\* Supported by the National Research Council of Canada.

<sup>1</sup> P. D. B. Collins and R. C. Johnson, *Phys. Rev.* **177**, 2472 (1969). A fuller set of references to earlier work can be found in this paper.

<sup>2</sup> An account of the background to this work can be found in P. D. B. Collins and E. J. Squires, *Regge Poles in Particle Physics* (Springer-Verlag, Berlin, 1968).

<sup>3</sup> G. F. Chew and C. E. Jones, *Phys. Rev.* **135**, B208 (1964).

<sup>4</sup> S. Mandelstam, *Phys. Rev.* **112**, 1344 (1958).

<sup>5</sup> G. Frye and R. L. Warnock, *Phys. Rev.* **123**, 1478 (1961).

<sup>6</sup> P. D. B. Collins and V. L. Teplitz, *Phys. Rev.* **140**, B663 (1965).

<sup>7</sup> P. D. B. Collins, *Phys. Rev.* **142**, 1163 (1966).

<sup>8</sup> P. D. B. Collins and R. C. Johnson, *Phys. Rev.* **169**, 1222 (1968).

<sup>9</sup> G. F. Chew, *Phys. Rev.* **140**, B1427 (1965).

<sup>10</sup> G. F. Chew and V. L. Teplitz, *Phys. Rev.* **136**, B1154 (1964).

just above the  $\rho$  mass. This produced a spurious bump in the  $t$ -channel total cross section which was not reproduced in the output  $s$ -channel cross section. Thus full crossing symmetry was not achieved.

It is a disadvantage of our method that we are unable to follow the trajectories above the  $\pi$ - $\pi$  threshold  $s_0$ , so that self-consistency can only really be imposed on  $\alpha(s)$  for  $s < s_0$ . We have made use of the results of Bali,<sup>11</sup> who calculated  $\text{Im}\alpha(t)$  by a different method (though not in a fully crossing-symmetric calculation), to improve the parametrization of the trajectory functions, and are thereby able to impose approximate equality on the  $s$ - and  $t$ -channel cross sections. This greatly narrows the range of acceptable bootstrap solutions.

In Sec. II, we review, for completeness, the equations of the unitarized strip approximation derived in Ref. 1, and discuss the parametrization of the Regge functions. In Sec. III the numerical results of the bootstrap are presented, and some conclusions concerning this sort of dynamics are drawn in Sec. IV.

### II. UNITARIZED STRIP APPROXIMATION

For brevity we shall assume that the reader is familiar with the discussion presented in Ref. 1, and here we only quote the more important equations, without derivation.

In the new strip approximation of Chew and Jones the strips of the double spectral function for a given trajectory are given by

$$\rho_{st}(s,t) = \Delta_s \left[ \frac{1}{2} \pi \Gamma(t) P_{\alpha(t)}(-1 - s/2q_t^2) \right] \theta(s - s_1), \quad (2.1)$$

where

$$\Gamma(t) = [2\alpha(t) + 1] \bar{\gamma}(t) (-q_t^2/\bar{t})^{\alpha(t)}, \quad (2.2)$$

where  $\alpha(t)$  is the trajectory,  $\bar{\gamma}(t)(\bar{t})^{-\alpha(t)} \equiv \gamma(t)$  is the reduced residue,  $s_1$  is the boundary of the strip, and  $\bar{t}$  is the usual scale factor.

Each of these strips contributes to the total amplitude

$$R^{s_1}(s,t) = \frac{1}{2} \Gamma(t) \left[ -\frac{\pi}{\sin \pi \alpha(t)} P_{\alpha(t)} \left( 1 + \frac{s}{2q_t^2} \right) - \int_{-4q_t^2}^{s_1} \frac{P_{\alpha(t)}(-1 - s'/q_t^2)}{s' - s} ds' \right], \quad (2.3)$$

and the Reggeized Born approximation to an amplitude of isotopic spin  $I$  in the  $s$  channel is

$$A^\pm(s,t) = \sum_i [R_i^{t_1}(s,t) + (-1)^I R_i^{u_1}(s,u)] \delta_{II_i} + \sum_j \beta(I, I_j) [R_j^{s_1}(t,s) + (-1)^I R_j^{u_1}(t,u)] + (-1)^I \sum_k \beta(I, I_k) [R_k^{s_1}(u,s) + (-1)^I R_k^{t_1}(u,t)], \quad (2.4)$$

where  $\beta(I, I_j)$  is the  $\pi$ - $\pi$  isotopic spin crossing matrix

<sup>11</sup> N. F. Bali, Phys. Rev. **150**, 1358 (1966).

and the sums are over all the trajectories in each of the three channels.

The elastic double spectral function in the  $s$  channel is calculated using the Mandelstam iteration formula. From the elastic unitarity condition we have

$$\rho_{st}^{\text{el}s}(s,t) = \frac{g(s)}{\pi q_s \sqrt{s}} \int \int_{K=0} dt_1 dt_2 \times \frac{D_t^\pm(s_+, t_1) D_t^\pm(s_-, t_2)}{K^{1/2}(t, t_1, t_2, s)}, \quad (2.5)$$

where

$$K(t, t_1; t_2, s) = [t^2 + t_1^2 + t_2^2 - 2(t t_1 + t t_2 + t_1 t_2) - t t_1 t_2 / q_s^2], \quad (2.6)$$

and  $s_+$  and  $s_-$  are points above and below (respectively) the  $s$  cut of  $D_t$ . The  $g(s)$  is the function which, as explained in Ref. 1, cuts off the double spectral function above  $s_1$ , viz.,

$$g(s) = 1/(1 + e^{(s-s_1)/\Delta}). \quad (2.7)$$

Also,

$$D_t^\pm(s,t) = \frac{1}{\pi} \int \frac{\rho_{st}^{\text{el}s}(s'',t)}{s'' - s} ds'' + D_t^{v\pm}(s,t), \quad (2.8)$$

where  $D_t^v$  is the  $t$  discontinuity across the  $t$  and  $u$  strips, i.e.,

$$D_t^v(s,t) = \Delta_t [2R^{s_1}(s,t)]. \quad (2.9)$$

Having calculated by iteration  $\rho_{st}^{\text{el}s}(s,t)$  for all  $t < s_1$ , we can use crossing symmetry to find the other "corner" double spectral functions, viz.,

$$\begin{aligned} \rho_{st}^{\text{el}t}(s,t) &= \rho_{st}^{\text{el}s}(t,s), \\ \rho_{tu}^{\text{el}t}(t,u) &= \rho_{st}^{\text{el}s}(t,u), \\ \rho_{tu}^{\text{el}u}(t,u) &= \rho_{st}^{\text{el}s}(u,t). \end{aligned} \quad (2.10)$$

The contribution of these pieces of the double spectral function to the amplitude is

$$A^\pm(s,t) = \frac{1}{\pi} \int \int \frac{\rho_{st}^{\text{el}t}(s'',t') \pm \rho_{su}^{\text{el}u}(s'',t')}{(s'' - s)(t' - t)} ds'' dt' + \frac{1}{\pi^2} \int \int \frac{\rho_{tu}^{\text{el}t}(t',u'') \pm \rho_{tu}^{\text{el}u}(u',t'')}{(u'' - u')(t' - t)} du'' dt', \quad (2.11)$$

and this is to be added to (2.4).

A partial-wave projection is then made of the sum of (2.4) and (2.11) to find the partial-wave amplitude  $B_i(s)$ . The part  $B_i^v(s)$ , the sum of the left-hand cut and the right-hand cut above  $s_1$ , is then isolated, i.e.,

$$B_i^v(s) \equiv \frac{1}{\pi} \int_{-\infty}^{s_L} \frac{\text{Im} B_i(s')}{s' - s} ds' + \frac{1}{\pi} \int_{s_1}^{\infty} \frac{\text{Im} B_i(s')}{s' - s} ds'. \quad (2.12)$$

The elastic  $s$ -channel double spectral functions [ $\rho_{st}^{el}(s,t)$ , etc.] are also used to calculate the inelasticity within the strip region in terms of the inelasticity parameter  $\eta_l(s)$  [see Eq. (4.18) of Ref. 1].

All of this is used as input to the  $N/D$  equations written in the Frye-Warnock form:

$$\bar{N}_l(s) = \bar{B}_l^v(s) + \frac{1}{\pi} \int_{s_0}^{s_1} \frac{\bar{B}_l^v(s') - \bar{B}_l(s)}{s' - s} \times \frac{\rho_l(s') \bar{N}_l(s')}{\eta_l(s')} ds' \quad (2.13)$$

and

$$D_l(s) = 1 - \frac{1}{\pi} \int_{s_0}^{s_1} \frac{\rho_l(s') \bar{N}_l(s')}{\eta_l(s') (s' - s)} ds', \quad (2.14)$$

where

$$\bar{B}_l^v(s) = B_l^v(s) + \frac{P}{\pi} \int_{s_0}^{s_1} \frac{1 - \eta_l(s')}{2\rho_l(s') (s' - s)} ds', \quad (2.15)$$

$$\bar{N}_l(s) = \frac{2\eta_l(s)}{1 + \eta_l(s)} \text{Re}\{N_l(s)\}, \quad (2.16)$$

and

$$\rho_l(s) = \left( \frac{s - 4m_\pi^2}{s} \right)^{1/2} \left( \frac{s - 4m_\pi^2}{4} \right)^l. \quad (2.17)$$

The output Regge parameters are then obtained from

$$D_{\alpha(s)}(s) = 0 \quad (2.18)$$

and

$$\frac{\gamma(s)}{\alpha'(s)} = \frac{N_\alpha(s)}{D_\alpha'(s)} \Big|_{l=\alpha(s)}, \quad (2.19)$$

where the primes denote  $d/ds$ . However, it is only possible to obtain  $\alpha(s)$  and  $\gamma(s)$  below threshold in this way, since above threshold the pole moves onto the unphysical  $s$  sheet, and we should need to solve the equations for complex  $l$  and  $s$ . As discussed in Ref. 1, this is the principal disadvantage of our method compared with the purely iterative calculation of, for example, Bali *et al.*<sup>11,12</sup>

The Regge functions are expected to satisfy dispersion relations of the form

$$\alpha(s) = \alpha(\infty) + \frac{1}{\pi} \int_{s_0}^{\infty} \frac{\text{Im}\alpha(s')}{s' - s} ds' \quad (2.20)$$

and

$$\gamma(s) = - \frac{1}{\pi} \int_{s_0}^{\infty} \frac{\text{Im}\gamma(s')}{s' - s} ds', \quad (2.21)$$

provided that two trajectories do not cross (which might introduce left-hand cuts<sup>2</sup>). The assumptions

implicit in (2.20) and (2.21) about the number of subtractions needed in these dispersion relations can be shown to follow from the form of the model.<sup>3,13</sup> In particular, we cannot have trajectories with (see Sec. IV)

$$\alpha(s) \rightarrow \pm \infty, \quad (2.22)$$

$$s \rightarrow \pm \infty.$$

In Ref. 1 we used a Breit-Wigner shape for  $\text{Im}\alpha$ , and adjusted the parameters until the form of the function below threshold agreed with the output from the  $N/D$  equations. The result was that  $D_l^v(s,t)$  from (2.9) obtained a spurious peak at the value of  $t$  corresponding to the maximum of  $\text{Im}\alpha(t)$  (which had to be just above the  $\rho$  mass in order to give adequate curvature to the trajectory). Such a peak was not, of course, found in the output cross section, and so proper crossing symmetry was not achieved.

An examination of Bali's calculations reveals what seems to be a more likely parametrization. It is evident from his Figs. 8 and 10 that  $\text{Im}\alpha$  in fact rises almost linearly throughout the strip, and is only really damped down by the cutting-off of elastic unitarity by  $g(s)$  in (2.5).

At first sight, this might seem to imply an inconsistency in the strip approximation, since if  $D_l^v(s,t)$  were to have its peak close to the boundary of the strip (i.e.,  $t \simeq s_1$ ) the first iteration of  $D_l^v(s,t)$  in (2.5) would produce a peak at  $t \simeq 4s_1$ , with further peaks for successive iterations, and a smooth Regge behavior would not be seen until  $t \gg s_1$ . The strip approximation requires Regge behavior for  $t > s_1$ , and experimentally Regge behavior is known to set in at quite low energies. In fact, however, even in Bali's potential-scattering calculations [where  $\text{Im}\alpha$  is eventually cut off by the  $\ln s/s$  convergence of  $B_l^v(s)$ ],  $\text{Im}\alpha(t)$  continues to rise up to energies large compared with the masses which determine the scale of the forces despite the fact that Regge behavior sets in at much lower energies than this.

The solution to this problem is that  $\gamma(t)$  is very small in the upper part of the strip. In Bali's calculations  $\text{Im}\gamma(t)$  is negative just above threshold, which pulls  $\text{Re}\gamma(t)$  down sharply in this region (see Fig. 6 of Ref. 11). It is evident from (2.9) that if  $|\gamma(t)|$  is small for  $t > m_\rho^2$  then so is  $|D_l^v|$ , and we can expect the double spectral function calculated by the iteration (2.5) to achieve a smooth Regge form by the time we have reached the boundaries of the strip (see Sec. III).

We therefore considered parametrizations of the form

$$\text{Im}\alpha(t) = \pi C_1 (t - t_B) \theta(t - t_B) \bar{\theta}(t_\alpha, \Delta, t), \quad (2.23)$$

where  $C_1$  is a constant,  $t_B \gtrsim 4m_\pi^2$  [adjusted to make  $\text{Im}\alpha(m_\rho^2)$  fairly small], and  $\bar{\theta}(t_\alpha, \Delta, t)$  is a cutoff function which is used to damp  $\text{Im}\alpha(t)$  exponentially to zero over a region of width  $\Delta$  around  $t = t_\alpha$ .

<sup>12</sup> N. F. Bali, G. F. Chew, and S. Y. Chu, Phys. Rev. **150**, 1352 (1966).

<sup>13</sup> C. E. Jones, Phys. Rev. **135**, B214 (1964).

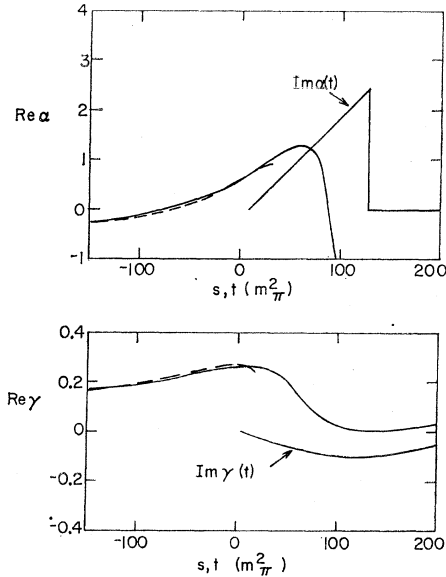


FIG. 1. Self-consistent  $\rho$ -meson trajectory and residue functions, with a linear form for  $\text{Im}\alpha(t)$ , and with  $\text{Re}\gamma(t)$  arranged to be small where  $\text{Im}\alpha(t)$  reaches its maximum. The input parametrizations are the full line, and the output is the dashed lines. The parameters are  $\alpha(\infty) = -0.34$ ,  $c_1 = 6.2 \times 10^{-3} m_\pi^{-2}$ ,  $t_B = 8 m_\pi^2$ ,  $t_\alpha = 127.2 m_\pi^2$ ,  $c_2 = 12.73$ ,  $\lambda = 0.1$ ,  $d = 275 m_\pi^2$ ,  $a_2 = 205 m_\pi^2$ ,  $b_2 = 130 m_\pi^2$ ,  $s_1 = 1000 m_\pi^2$ , and  $\Delta = 5 m_\pi^2$ .

Bali's work suggests  $t_\alpha \sim s_1$ , with  $|\text{Re}\gamma(t)|$  small near the peak of  $\text{Im}\alpha(t)$  at  $t \lesssim t_\alpha$ . However, examination of the numerical  $N/D$  solutions reveals that without superconvergence constraints on  $B_l^v(s)$  (see Sec. V), it is impossible to get  $\alpha_p(\infty)$  below about  $-0.35$ . If we insert this value in (2.20) and choose parameters for  $\text{Im}\alpha(t)$  in (2.23) such that  $\text{Re}\alpha(t=m_\rho^2) \approx 1$ , we find that the resultant trajectory is very flat for  $t \approx 0$ . This flatness is not characteristic of our output trajectories. It would seem therefore that unlike Bali's calculation, our  $\text{Im}\alpha$  is being cut off for  $s \ll s_1$ . We thus take  $t_\alpha$  to be a free parameter which we adjust until the input and output trajectories match as well as possible near  $t=0$ . We shall see in Sec. III that rather small values of  $t_\alpha$  ( $t_\alpha \ll s_1$ ) are called for. This has the benefit that the output trajectories have roughly the same sort of slope at  $t=0$  as is found in phenomenological fits.

To suppress spurious bumps in  $D_l^v(s, t)$ , the parametrization of  $\text{Im}\gamma(t)$  is adjusted so that  $|\text{Re}\gamma(t)|$  is very small where  $\text{Im}\alpha(t)$  reaches its maximum, i.e., for  $t = t_\alpha$ . A suitable form is that used in Ref. 1, namely,

$$\text{Im}\gamma(t) = \frac{c_2 x^\lambda (x-d)}{(x-a_2)^2 + b_2^2}, \quad x = t - 4m_\pi^2. \quad (2.24)$$

The cutoff function  $\bar{\theta}$  in  $\text{Im}\alpha(t)$  is chosen to be of the form

$$\bar{\theta}(t_\alpha, \Delta, t) = (1 + e^{(t-t_\alpha+2\Delta)/\Delta})^{-1}. \quad (2.25)$$

Thus, for each trajectory we have nine free parameters  $\alpha(\infty)$ ,  $c_1$ ,  $t_B$ ,  $t_\alpha$ ,  $c_2$ ,  $\lambda$ ,  $d$ ,  $a_2$ , and  $b_2$ , as well as the two

"cutoff" parameters  $s_1$  and  $\Delta$ , and the scale factor  $\bar{t}$ , which is held fixed at  $200 m_\pi^2$ . The object is to solve the equations of this section with as many trajectories as are needed for self-consistency in  $\pi$ - $\pi$  scattering, and to check that the choice of  $s_1$  and  $\Delta$  is not of great importance. In Sec. III we describe our numerical results.

### III. SELF-CONSISTENT TRAJECTORIES

In Fig. 1 we show a self-consistent  $\rho$  trajectory with the new parametrization. Evidently, there is good agreement between the input and output trajectory and residue functions below threshold. Figure 2 shows that the corresponding partial-wave cross sections do not agree so well, however, and the widths of the input and output  $\rho$  disagree by a factor of 2. Two encouraging improvements of these results over those of Ref. 1 are that  $\alpha(\infty)$  is much lower, giving a steeper trajectory with the physical intercept (0.57),<sup>14</sup> and secondly that the requirement that  $|\text{Re}\gamma(t)|$  be small where  $\text{Im}\alpha(t)$  is peaked imposes a fairly stringent condition on the parameters of  $\gamma(t)$ , and leads to a much more nearly unique bootstrapped  $\rho$  trajectory. The extreme values of  $\alpha_p(0)$  for which we were able to find self-consistent solutions with satisfactory crossing symmetry (i.e., with no unacceptable structure in the  $t$ -channel cross section) were 0.3 and 0.72.

In (2.13) the parameter  $s_1$  is the point where Regge asymptotic behavior takes over from the low-energy resonance strip region, and, as discussed in Ref. 15, both  $N$  and  $D$  have logarithmic singularities there. On the other hand, in (2.5) we have cut off unitarity more gently at  $s_1$  in calculating the double spectral function, and so in Fig. 3 we show the effect of using the same cutoff in the  $N/D$  equations, i.e., we replace  $\rho_l(s)$  in (2.13) by

$$\bar{\rho}_l(s) = \rho_l(s) (1 + e^{(s-s_1)/\Delta})^{-1}.$$

Evidently this slightly more consistent procedure makes very little quantitative difference.

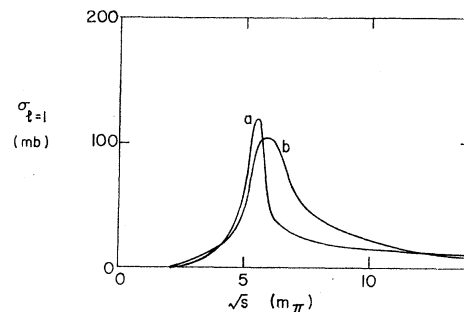


FIG. 2. (a) Input ( $t$ -channel) and (b) output ( $s$ -channel) cross sections in the  $I=l=1$  state, showing the self-consistent  $\rho$ -meson resonances for the case given in Fig. 1. The input and output  $\rho$  widths are  $\Gamma_{\text{in}} = 135$  MeV and  $\Gamma_{\text{out}} = 265$  MeV.

<sup>14</sup> See, e.g., G. Höhler, H. Schaile, and P. Sonderegger, Phys. Letters **20**, 79 (1966).

<sup>15</sup> G. F. Chew, Phys. Rev. **130**, 1264 (1964).

Just as in the  $\rho$  bootstrap described in Ref. 1, to get self-consistency a large residue is necessary. Indeed it is necessary in the present work to use input residues which are larger than those in Ref. 1, in order to have  $\alpha_\rho(\infty) < 0$  with  $\alpha_\rho(0) = 0.57$  and  $\text{Re}\alpha_\rho(30) = 1$ , since with the new parametrization of  $\alpha(t)$  only a limited curvature of  $\text{Re}\alpha(t)$  is permitted. With large residues, crossed-channel unitarity is violated for  $l < 0.3$ , compared with  $l < 0.2$  in Ref. 1.

The nature of the  $\pi$ - $\pi$  crossing matrix ensures that the  $\rho$ -exchange force generates an output trajectory in the  $I=0$  channel which lies higher than the  $\rho$ . This we identify with the  $P$ , and remark that  $\pi$ - $\pi$  dynamics gives perhaps the best evidence for the supposition that there is a high-lying Regge pole with the usual sort of slope and vacuum quantum numbers.

Thus, for self-consistency, we must include both  $\rho$  and  $P$  in the crossed channels.

Figure 4 shows a self-consistent solution with both  $P$  and  $\rho$ . The two trajectories are almost parallel (the  $P$  is marginally the steeper), differing essentially only in their asymptotic values [ $\alpha_P(\infty) = 0.15$ ,  $\alpha_\rho(\infty) = -0.34$ ], and intercepts at  $t=0$ . The  $\rho$  has  $\alpha_\rho(0) = 0.55$  if the  $P$  saturates but does not exceed the unitarity bound  $\alpha_P(0) = 1.0$ . Again the restrictions imposed on the input residue parameters by demanding self-consistency both of the trajectories below threshold, and of the cross sections above threshold, permit only a relatively small range of bootstrap solutions. The extrema are given in Table I. It appears that the inclusion of the  $P$  force slightly narrows the range of acceptable  $\alpha_\rho(0)$  to between 0.32 and 0.69. If we demand the phenomenological value  $\alpha_\rho(0) = 0.57$ ,<sup>14</sup> we get  $\alpha_P(0) = 1.1$ .

It is by no means trivial that there is any acceptable solution, let alone a reasonably unique one, because in earlier calculations, using just the first Born approximation to the left-hand cut, the presence of the strong repulsion from  $P$  exchange produced nonsensical results (see Ref. 7). Iteration of the potential has corrected this, and has produced perfectly sensible output trajectories. The proper inclusion of the  $P$  has had the desirable results of making the self-consistent trajectories slightly steeper, and the residues smaller and falling off more rapidly as  $t \rightarrow -\infty$ . This is partly because after iteration there is a net attraction from the  $P$ ,

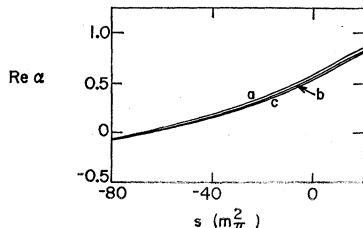


FIG. 3. Effects on the output trajectory of Fig. 1 of cutting off the  $N/D$  integrals of Eqs. (2.13) and (2.14) using a modified phase-space factor, as described in the text. The three cases are for (a)  $\Delta = 0$ , (b)  $\Delta = 5m_\pi^2$ , and (c)  $\Delta = 10m_\pi^2$ .

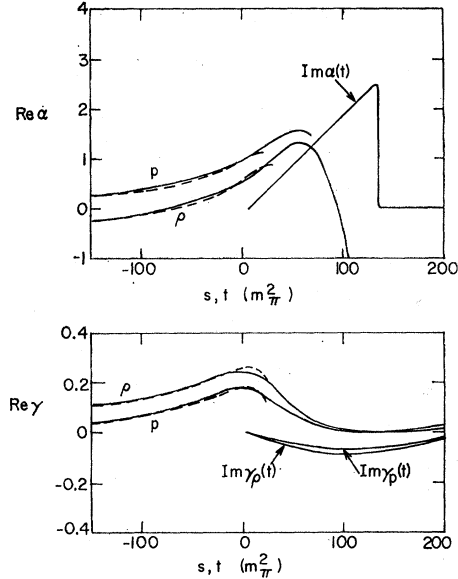


FIG. 4. Self-consistent  $\rho$  and Pomeranchuk trajectory and residue functions, in each case with a linear form for  $\text{Im}\alpha(t)$ , and with  $\text{Re}\gamma(t)$  arranged to be small where  $\text{Im}\alpha(t)$  reaches its maximum. Input is the full line, and output the dashed line. Since the output trajectories residues are almost parallel, the  $P$  and  $\rho$  have the following input parameters in common:  $t_B = 8m_\pi^2$ ,  $c_1 = 1.4 \times 10^{-3}m_\pi^{-2}$ ,  $t_a = 135.8m_\pi^2$ ,  $\lambda = 0.1$ ,  $\Delta = 5m_\pi^2$ ,  $s_1 = 1000m_\pi^2$ ,  $d = 212m_\pi^2$ ,  $a_2 = 208m_\pi^2$ , and  $b_2 = 182m_\pi^2$ ; they differ in the parameters  $\alpha_\rho(\infty) = -0.35$ ,  $\alpha_P(\infty) = 0.15$ ,  $c_2^P = 11.33$ , and  $c_2^\rho = 8.20$ .

so that the attractive force needed from the  $\rho$  can be reduced. Also the repulsive part of the  $P$  reduces  $B_i^*(s)$  near threshold (see Fig. 5) and hence decreases  $N_i(s)$ . In turn, this reduces the width of the output  $\rho$  through (2.19).

The input and output partial-wave cross sections are compared in Fig. 6, and it is seen that a tolerable (though not perfect) self-consistency has been achieved. It is particularly gratifying that a symmetrical resonance shape has been obtained. The output  $\rho$ -meson width of 155 MeV is only a few percent greater than the most likely physical value,<sup>16</sup> and a good deal better than has resulted from previous efforts.<sup>2</sup>

The results are almost independent of  $s_1$ , provided that it is greater than about  $1000m_\pi^2$ , as Fig. 7 shows, and we feel justified in ceasing to regard it as a parameter of the model. Figures 8 and 9 demonstrate that a

TABLE I. Extreme values of the  $P$  and  $\rho$  trajectory intercepts possible for a crossing-symmetric bootstrap solution. Also given are the corresponding trajectory slopes, in units of  $\text{GeV}^{-2}$ .

	$\alpha_P(0)$	$\alpha_P'(0)$	$\alpha_\rho(0)$	$\alpha_\rho'(0)$
Upper	1.20	1.02	0.69	1.00
Lower	0.89	0.72	0.32	0.69

<sup>16</sup> N. Barash-Schmidt, A. Barbaro-Galtieri, L. R. Price, A. H. Rosenfeld, P. Söding, C. G. Wohl, and M. Roos, Rev. Mod. Phys. 41, 109 (1969).

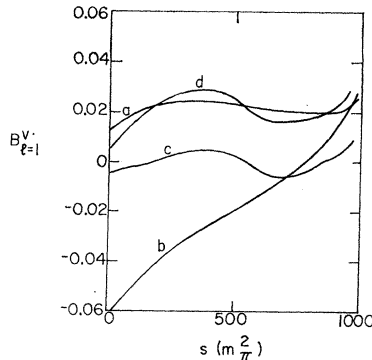


FIG. 5. The potential function  $B_l^\nu(s)$ , defined in (2.12), for  $l=1$  with the exchanged  $\rho$  and  $P$  parameters as for the self-consistent case shown in Fig. 4. The four curves correspond to the following potentials: (a) iterated  $\rho$  exchange alone, (b)  $P$  exchange in the first Born approximation, (c) iterated  $P$  exchange alone, and (d) the total potential (a)+(c) that produces the output trajectories of Fig. 4.

fair matching of the high- and low-energy parts of the amplitude has been attained. With more trouble (and a good deal more computer time) an exact matching could probably be achieved.

There is a good deal of evidence that secondary  $I=0$  and  $I=1$  trajectories ( $P'$ ,  $\rho'$ , etc.) are coupled to the  $\pi$ - $\pi$  system but in this calculation there was no sign of such poles, even when they were included in the input. Presumably, if they exist they must be generated in other channels.

#### IV. CONCLUSION

It has proved possible to bootstrap the  $\rho$  and  $P$  trajectories in the  $\pi$ - $\pi$  system, and to obtain trajectories which are quite close to the physical trajectories in their behavior near  $t=0$ . The difficulty of previous calculations, that the  $P$  repulsion gives nonsensical results, has been overcome by iterating the potential, and as expected it results in smaller  $\rho_a$  widths. The input and output widths are in fair agreement (the agreement could probably be improved, but with an order of magnitude more trouble), and are within a small fraction of the

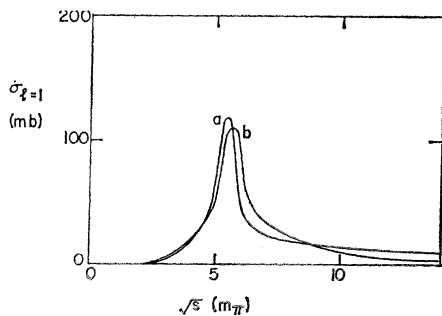


FIG. 6. (a)  $s$ - and (b)  $t$ -channel cross sections in the state  $I=l=1$  for the self-consistent crossing symmetric solution of Fig. 4. The input and output  $\rho$  widths are  $\Gamma_{in}=135$  MeV and  $\Gamma_{out}=135$  MeV.

physical width. This is much better than has been achieved by such calculations previously. Also the end points of the trajectories are lower, and the slopes close to those found empirically.<sup>14</sup>

Self-consistency does not restrict the trajectories uniquely, but the range of reasonable self-consistent trajectories is comparatively narrow. The results are independent of the strip width  $s_1$ , which does not act as a cutoff, but is simply the matching point between the high- and low-energy regions.

Despite this modicum of success there remain considerable difficulties with the whole bootstrap hypothesis, because there is now some evidence that meson trajectories remain straight over quite a large range of energy, producing several recurrences for  $s>0$ , and cutting several negative integers for  $s>0$ , where they result in nonsense dips.<sup>2</sup> It may be that the addition of higher threshold channels, which include external particles with spin, is capable of keeping trajectories rising, as Mandelstam<sup>17</sup> has suggested (see also Ref. 2), but this is by no means obvious since the "forces" between particles with spin must satisfy superconvergence conditions if unitarity is not to be violated. Otherwise, if the total spin of the channel were  $S$  the trajectories would have  $\alpha(\infty)=S-1$ , due to the Gribov-Pomeranchuk<sup>18</sup> singularity in the potential at  $l=1$ , and this violates the Froissart bound for  $S>2$ . The effect of such superconvergence conditions will be to weaken the forces. Similarly, if the trajectories are to pass through

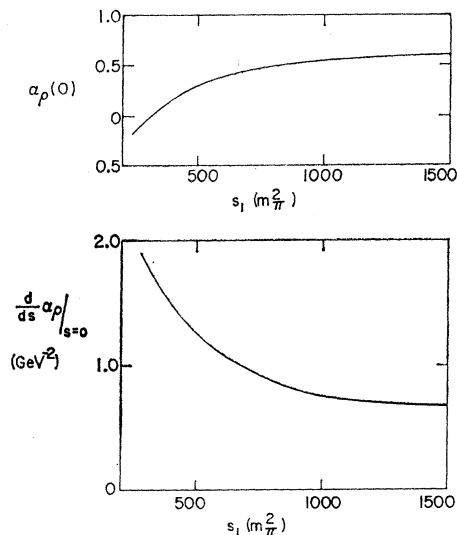


FIG. 7. Values of  $\alpha_\rho(s=0)$  and  $d\alpha_\rho(s)/ds|_{s=0}$  plotted against  $s_1$ , the strip width, with all other parameters held fixed at those quoted in Fig. 4.

<sup>17</sup> S. Mandelstam, in *1966 Tokyo Summer Lectures in Physics*, edited by G. Takeda and A. Fujii (W. A. Benjamin, Inc., New York, 1966), Part II; also, *Phys. Rev.* **168**, 1539 (1968).

<sup>18</sup> V. N. Gribov and I. Ya Pomeranchuk, in *Proceedings of the International Conference on High Energy Physics, Geneva, 1962*, edited by J. Prentki (CERN, Geneva, 1962), p. 522.

negative integer values of  $\alpha$ , more superconvergence conditions must be imposed, with a further weakening effect.

We have argued in a previous paper<sup>19</sup> that if continuously rising trajectories are to be bootstrapped, or indeed calculated in any sort of "equivalent-potential" calculation,  $\text{Im}\alpha(s)$  must be an increasing function of  $s$ . This seems to be in disagreement with the experimental facts, at least for mesons. For, if the  $R$  and  $T$  mesons are on the  $\rho$  trajectory, their small widths show that  $\text{Im}\alpha$  is decreasing at energies above the  $\rho$  mass. We then have no hope of bootstrapping the trajectory. The quark model (or some other model which makes very high threshold channels dominant) might succeed by requiring  $\text{Im}\alpha$  to be large above the two-quark threshold. However, then the  $\rho$  would be a CDD (Castillejo-Dalitz-Dyson) pole in the  $\pi\pi$   $l=1$  partial wave, and we would not expect to be able to generate it in this sort of calculation. The comparative success of our computations may thus be regarded as (rather weak) evidence against such a quark model.

The other alternative discussed in Ref. 19 is that the slopes of the Regge trajectories are arbitrary parameters of the  $S$  matrix, which have to be inserted *a priori* into

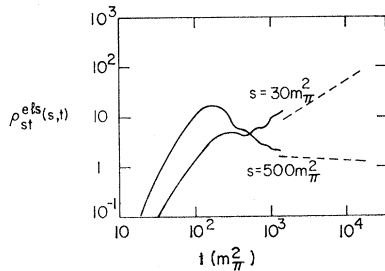


FIG. 8. Plot of the iterated double spectral function  $\rho_{st}^{e^{is}(s,t)}$  against  $t$  at fixed  $s$  for the case of Fig. 4. At  $s_1 (=1000m_\pi^2)$  the iterated double spectral function matches onto the  $s$ -channel strip contribution fairly well.

<sup>19</sup> P. D. B. Collins, R. C. Johnson, and E. J. Squires, Phys. Letters **26B**, 223 (1968).

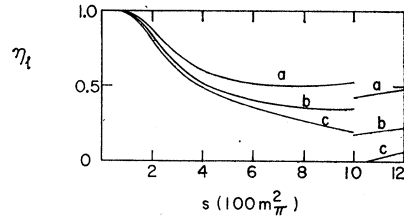


FIG. 9. Inelasticity parameter  $\eta_l(s)$  for  $l=1$  as a function of  $s$  for (a)  $l=1$ , (b)  $l=0.5$ , and (c)  $l=0.3$ , with the parameters of Fig. 4. At  $s_i$  it matches reasonably the values calculated from the asymptotic strip, but unitarity is violated for  $l<0.3$ .

one's calculations. So instead of (2.20) we have the dispersion relation

$$\alpha(s) = a + bs + \frac{1}{\pi} \int_{s_0}^{\infty} \frac{\text{Im}\alpha(s')}{s' - s} ds'. \quad (4.1)$$

There might, for instance, be a universal slope,  $b$ , of about  $1 \text{ GeV}^{-2}$ , with the dynamics (which is essentially contained in  $\text{Im}\alpha$ ) responsible only for local variations from this in the various physical trajectories. But again the comparative success of our calculations in obtaining a reasonable slope for the trajectories near  $l=0$  argues against such a hypothesis.

It still seems reasonable to hope that the sort of calculations we have performed, if extended by the inclusion of more channels and the removal of the Gribov-Pomeranchuk singularities at  $l = -1, -2$ , etc., may give a good account of trajectories for small  $|s|$ . But it will obviously involve an inordinate amount of computation to generalize calculations with this sort of sophistication to include many coupled channels. And our results prove that the much simpler, and therefore more readily generalizable, models of the past, which used the first Born approximation with a non-Reggeized exchange, and simply cut off the unitarity integral, represent very unsatisfactory approximations to the dynamics. It is clearly going to be very difficult to make a really critical test of the bootstrap hypothesis.